Psoralen Photo-Cross-Linking by Triplex-Forming Oligonucleotides at Multiple Sites in the Human Rhodopsin Gene†

Brian D. Perkins, Theodore G. Wensel, Karen M. Vasquez,‡ and John H. Wilson*

Verna and Marrs McLean Department of Biochemistry, Baylor College of Medicine, One Baylor Plaza, Houston, Texas 77030

Received February 4, 1999; Revised Manuscript Received July 19, 1999

ABSTRACT: Targeting DNA damage by triplex-forming oligonucleotides (TFOs) represents a way of modifying gene expression and structure and a possible approach to gene therapy. We have determined that this approach can deliver damage with great specificity to sites in the human gene for the G-protein-linked receptor rhodopsin, mutations of which can lead to the genetic disorder autosomal dominant retinitis pigmentosa. We have introduced DNA monoadducts and interstrand cross-links at multiple target sites within the gene using TFOs with a photoactivatable psoralen group at the 5′-end. The extent of formation of photoadducts (i.e., monoadducts and cross-links) was measured at target sites with a 5′-ApT sequence at the triplex−duplex junction and at a target site with 5′-ApT and 5′-TpA sequences located four and seven nucleotides away, respectively. To improve psoralen reactivity at more distant sites, psoralen moieties were attached to TFOs with nucleotide "linkers" from two to nine nucleotides in length. High-affinity binding was maintained with linkers of up to 10 nucleotides, but affinities tended to decrease somewhat with increasing linker length due to faster dissociation kinetics. DNase I footprinting indicated little, if any, interaction between linkers and the duplex. Psoralen−TFO conjugates formed DNA cross-links with high efficiency (56−65%) at 5′-ApT sequences located at triplex junctions. At a 5′-ApT site four nucleotides away, the efficiency varied with linker length; a four-nucleotide linker gave the highest efficiency. Duplexes with 5′-TpA and 5′-ApT sites two nucleotides away, in otherwise identical sequences, were cross-linked with efficiencies of 56 and 38%, respectively. These results indicate that TFO−linker−psoralen conjugates allow simultaneous, efficient targeting of multiple sites in the human rhodopsin gene.

Rhodopsin is the G-protein-coupled receptor of the visual signal transduction cascade (*1*), and more than 70 rhodopsin mutations are associated with the disease autosomal dominant retinitis pigmentosa (ADRP),[1] making it the most common cause of ADRP (*2*). This disease affects approximately 1.5 million people worldwide (*3*) and is characterized by photoreceptor cell death and retinal degeneration that ultimately results in blindness (*4*). Physiological results from mice with a rhodopsin heterozygous null mutation (*5*) and the presence of a rhodopsin null mutation in haploid carriers without RP (*6*) suggest that ADRP is not caused by haploinsufficiency, but rather by the harmful expression of mutant rhodopsin. To treat ADRP, as well as similar dominant disorders, it is necessary to develop technologies that inactivate, repair, or replace the defective copy of the gene.

One possible approach is triplex DNA technology (*7*), which can successfully deliver DNA damaging agents in a site-specific manner, thereby altering the expression or structure of mammalian genes using triplex-forming oligonucleotides (TFOs). Triplex formation occurs when an oligonucleotide binds to duplex DNA through the major groove and forms specific hydrogen bonds with the purine-rich strand of a target duplex. TFOs have been used to inhibit expression of both plasmid (*8*−*11*) and chromosomal gene targets (*11*−*21*) inside cells. TFOs covalently linked to DNA-damaging agents have been used to direct localized mutations to plasmid (*22*−*24*) and chromosomal targets in mammalian cells (*25*) and increase the level of homologous recombination (*26*, *27*) on plasmid targets in mammalian cells.

The photoactivatable psoralen molecules constitute a well-characterized class of DNA-damaging agents (*28*) and are often attached to TFOs to induce site-specific DNA damage at pyrimidines adjacent to the triplex binding site. The mechanism of psoralen action is well-understood (*28*). Briefly, the absorption of one photon causes the formation of a covalent monoadduct with a pyrimidine in one strand of the nucleic acid, and the absorption of a second photon converts the monoadduct to an interstrand cross-link with an adjacent pyrimidine in the opposite strand. Free psoralen reacts with DNA in a sequence-dependent manner with the preferred order being 5′-TpA > 5′-ApT ≫ 5′-TpG > 5′-GpT (*29*), though the surrounding sequence context appears to have some effect on psoralen reactivity (*30*−*32*); however, the sequence specificity of psoralens conjugated to TFOs has not been directly measured. DNA damage caused by psoralen−TFO conjugates may result in double-strand breaks, which are known to stimulate recombination several

† This work was funded by grants from the Texas Advanced Technology Program (004949-803) and the NIH (EY11731). B.D.P. is supported by a training grant from NIH (T32 EY07102).

* Corresponding author.

‡ Current address: Department of Therapeutic Radiology, Yale University School of Medicine, New Haven, CT 06510.

[1] Abbreviations: TFO, triplex-forming oligonucleotide; ADRP, autosomal dominant retinitis pigmentosa; PAGE, polyacrylamide gel electrophoresis; UVA, ultraviolet-A light.

10.1021/bi9902743 CCC: $18.00
Published on Web 09/09/1999

1000-fold in regions surrounding the break (*33*, *34*). Psoralen-conjugated TFOs have also been used to induce small deletions, thereby inactivating gene function (*25*). The use of psoralen-conjugated TFOs to inhibit gene expression, induce mutations, and enhance recombination may be exploited to inactivate or correct defective genes.

We are testing the human rhodopsin gene as a target for triplex-based approaches to gene therapy. We have previously characterized the binding of TFOs to multiple sites in the human rhodopsin gene (*35*). In this paper, we describe the in vitro use of psoralen-conjugated TFOs in causing damage at specific sites in the rhodopsin gene. We have identified five target sites with a psoralen cross-linking site at or near ($\leq$10 bp) the triplex binding site on the 3′-end of the purine-rich strand. Using psoralen-conjugated TFOs, we have achieved efficient cross-linking at the triplex junction. We have also used TFOs with psoralen moieties attached via nucleotide linkers and observe site-specific cross-linking at sequences distant from the triplex binding site. During the course of these studies, we have investigated the interactions of linkers with the duplex and their effects on binding affinity and kinetics, and we have determined the relative reactivity of psoralen TFOs with 5′-TpA and 5′-ApT sites in identical sequence contexts.

EXPERIMENTAL PROCEDURES

Oligonucleotide Synthesis and Purification. Unmodified oligodeoxyribonucleotides were purchased from Integrated DNA Technologies, Inc. (Coralville, IA). TFOs were dissolved in Milli-Q water and desalted on NAP-5 columns (Pharmacia LKB Biotechnology, Uppsala, Sweden). Oligonucleotides were then purified by denaturing PAGE (15% acrylamide) as described previously (*36*). The oligonucleotide purity was analyzed by PAGE of 5′-end-labeled oligos. Oligos were labeled using T4 polynucleotide kinase (New England Biolabs Inc., Beverly, MA) and [γ-^{32}P]ATP (6000 Ci/mmol) (New England Nuclear Research Products, Boston, MA) for 30 min at 37 °C. Gel-purified psoralen-modified TFOs were purchased from Oligos Etc. (Wilsonville, OR). They were 3′-end-labeled using terminal deoxynucleotidyl transferase (Gibco, Rockville, MD) with [α-^{32}P]dideoxyATP (Amersham Pharmacia, Uppsala, Sweden) and examined for purity by denaturing PAGE. All exhibited a single species and were used without further purification. For all TFOs, the psoralen derivative, 4′-(hydroxymethyl)-4,5′,8-trimethylpsoralen (HMT), was joined to the TFO via a six-carbon (C-6) linker. DNA concentrations were determined by UV absorbance at 260 nm.

Triplex Formation by Electrophoretic Mobility Shift Assay with Synthetic Duplexes. Oligonucleotides corresponding to gene target sites were annealed in a 1:1 molar ratio to form a target duplex. Duplex strands were 5′-end-labeled using T4 polynucleotide kinase and [γ-^{32}P]ATP, and the duplex was then gel purified by PAGE (12% acrylamide) under nondenaturing conditions. Labeled duplex ($<1 \times 10^{-10}$ M) was incubated with increasing concentrations of TFO in binding buffer [10 mM Tris-HCl (pH 7.6), 10 mM $MgCl_2$, and 10% sucrose] at 37 °C for 72 h to attain equilibrium (*36*, *37*). Triplex-induced mobility shifts were monitored by electrophoresis through native 12% polyacrylamide gels containing 89 mM Tris-borate (pH 8.0) and 10 mM $MgCl_2$. Gels were run for 6−7 h at 55 V and 22 °C, dried, and examined by autoradiography.

Kinetics of Triplex Dissociation. Dissociation kinetics were measured by initially incubating the labeled duplex ($\sim 5 \times 10^{-8}$ M) with TFO at high concentrations (2×10^{-6} M) in triplex binding buffer at 37 °C for 15 h to drive triplex formation. Following incubation, the reaction mixtures were diluted in triplex binding buffer to a final duplex concentration of 2×10^{-11} M and a final TFO concentration of 4×10^{-9} M. The triplexes were allowed to dissociate for the indicated times with triplex dissociation followed by electrophoresis, as described above, and quantitation by PhosphorImager (Molecular Dynamics, Sunnyvale, CA) analysis using ImageQuant software.

DNase I Footprinting Analysis. Oligonucleotides corresponding to the target site were annealed in a 1:1 molar ratio to form a target duplex, with the purine-rich strand of the duplex radiolabeled. The purine-rich strand was 5′-end-labeled using T4 polynucleotide kinase and [γ-^{32}P]ATP, and following annealing, the duplex was gel purified. The 5′-end-labeled synthetic duplex was incubated with TFO in triplex binding buffer at 37 °C in a final volume of 10 μL for 24 h. DNase I at a concentration of 0.0125 unit/mL was then added, and samples were incubated at room temperature for 4 min. Ten microliters of stop solution/loading dye [formamide, 2% bromophenol blue (w/v), and 140 mM EDTA] was subsequently added. Samples were immediately denatured at 95 °C for 5 min and subjected to electrophoresis on 15% polyacrylamide denaturing gels containing TBE [89 mM Tris-borate (pH 8.0) and 2 mM EDTA], dried, and autoradiographed. Duplexes were treated with DMS and piperidine to produce a G-ladder as described previously (*38*).

Photoadduct Formation and Analysis. Oligonucleotides corresponding to target sites were annealed in a 1:1 molar ratio to form a target duplex. Duplexes were 5′-end-labeled to high specific activity with [γ-^{32}P]ATP and gel purified. Duplex (at a final concentration of 3×10^{-10} M) was incubated for 24 h with 1×10^{-6} M psoralen−TFO conjugates in triplex binding buffer at 37 °C. Triplex formation reactions in which psoralen−TFO conjugates were used were set up in a dark room using only dim red illumination from a photographic safe light. Following incubation, the samples were irradiated with UVA for the periods of time indicated in the figure legends. The light source was an 8 W handheld lamp (UVP, Upland, CA) emitting approximately 0.12 J/cm^2 per minute based upon measurement with a UVX radiometer (UVP). For samples irradiated for 60 min, 5 μL of Milli-Q water was added after 30 min to ensure minimal effects of evaporation over the course of the experiment. After irradiation, 10 μL of stop solution was added to the samples, which were then denatured at 95 °C prior to analysis by electrophoresis through 15% denaturing polyacrylamide gels containing TBE. The gels were subsequently dried and autoradiographed. Radioactivity was quantified using a PhosphorImager. Self-association and self-reaction of psoralen-modified TFOs was assessed by incubating 3′-end-labeled TFOs at various concentrations in the presence and absence of unlabeled target duplex, irradiating with UVA, and analyzing the products by electrophoresis on 15% polyacrylamide

Table 1: Triplex Target Sequences with Psoralen Cross-Linking Sites in Close Proximity

Duplex[a] [Site][b] (TFO)[c]	Target Sequence[d]
2 [1206] (TFO2)	5′ GACAGGGGCT**GAGAGGGGAGGCAGAGGA**TGCCAGAGGG 3′ 3′ CTGTCCCCGA**CTCTCCCCTCCGTCTCC**TACGGTCTCCC 5′
3 [1411] (TFO3)	5′ AAACTGAGGC**AGGGAGAGGGGAAGAGA**CTCATTTAGG 3′ 3′ TTTGACTCCG**TCCCTCTCCCCTTCTCT**GAGTAAATCC 5′
5 [1965] (TFO5)	5′ TTCATTTCCC**GAGAAGGGAGAGGGAGGAAGGA**CTGCCAATTC 3′ 3′ AAGTAAAGGG**CTCTTCCCTCTCCCTCCTTCCT**GACGGTTAAG 5′
9 [3135] (TFO9)	5′ TAGCAAGACT**GAGGAGGAAAGGGAAGTGAGAGTGGGAA**TTTTCTGGAG 3′ 3′ ATCGTTCTGA**CTCCTCCTTTCCCTTCACTCTCACCCTTA**AAAGACCTC 5′
15 [5313] (TFO15)	5′ GGCTGTGGCT**GGGGGAAGGTGTAGGGGATGGGAGA**CGCCTATAGT 3′ 3′ CCGACACCGACCCCCTTCCACATCCCCTACCCTCTGCGGATATCA 5′

[a] Numbers refer to the target sites in the rhodopsin gene (*35*). [b] Numbers in brackets refer to the most 5′ nucleotide of the target sequence in the RNA transcript. [c] TFOs in parentheses are targeted to the associated target sequences. [d] Target sequences are shown in boldface type. Proposed psoralen cross-linking sites are underlined. In this study, only TFOs with a 5′-conjugated psoralen were used; therefore, possible cross-linking sites on the 5′-side of the purine-rich strand of the target are not listed.

denaturing gels as described above. Radioactivity in various species was measured and quantified using a PhosphorImager.

RESULTS

Selection of Triplex Target Sites Capable of Photoadduct Formation. We originally identified eight triplex target sites within the rhodopsin gene capable of binding a TFO with high affinity ($K_d \leq 1 \times 10^{-8}$ M) under our standard conditions (*35*). Of these, five target sites had a preferred psoralen cross-linking sequence, 5′-TpA or 5′-ApT (*28*), within 10 bp of the 3′-end of the purine-rich strand in the target (Table 1). Two of these target sites, 1206 and 3135 (numbering refers to the position relative to the *Bam*HI site just upstream of the first exon, GenBank accession number K02281), had a psoralen cross-linking site located at the triplex−duplex junction (Table 1), whereas the other cross-linking sites were located at least four nucleotides away from the last base in the target sequence.

Since psoralen attached by a C-6 linker does not effectively cross-link such distant sites (*39*), we explored the use of additional nucleotides in extending psoralen for more efficient interaction at distant sites. Preliminary data with a target site in the APRT gene indicated that up to 10 additional nucleotides could be added with only a modest decrease in binding affinity. To test the ability of such nucleotide "linkers" to increase the extent of psoralen cross-linking at distant sites, we chose target site 1411 (Table 1). This site had a 5′-ApT site four nucleotides from the triplex junction and a 5′-TpA site seven nucleotides from the junction and is bound with high affinity by both GA− and GT−TFO conjugates (*35*).

Design and Binding Affinity of "Linker" TFOs. Two approaches were used to design nucleotide linkers in the hope of maximizing binding affinity and photoadduct formation. In one approach, the linker nucleotides at GA− and GT−TFO conjugates were designed using the standard rules of triplex formation by antiparallel, purine-rich TFOs, with G versus GC, T or A versus AT, T versus CG, and C versus TA base triplets (*7*, *40*) (Table 2; TFO3B−TFO3K). To reduce the potential for secondary structure within TFOs with linkers longer than six nucleotides, we positioned a T rather than a C over the T·A base pair at nucleotide 6 in the linker region (Table 2). In a second approach, linkers were designed to utilize the potential for alternate-strand triplex formation (*41*−*43*). In this approach, the linker nucleotides are designed to bind to the purines that flank the pyrimidine-rich segment of the target site; nucleotides were chosen on the basis of the standard rules for parallel triplex formation by pyrimidine-rich TFOs with C versus GC, T versus AT, T or C versus CG, and G versus TA base triplets (*7*) (Table 2; TFO3L−TFO3W). Thus, in the target region, these alternate-strand TFOs bind in an antiparallel orientation, whereas in the linker region, they have the potential to bind in a parallel arrangement.

Table 2: Sequences and Linker Lengths of TFOs Used in This Study

TFO	Sequence[a]	Linker Length[b]
	5′ AAACTGAGGC**AGGGAGAGGGGAAGAGA**CTCATTTAGG 3′ 3′ TTTGACTCCG**TCCCTCTCCCCTTCTCT**GAGTAAATCC 5′	
TFO3AT	3′ **TGGGTGTGGGGTTGTGT** 5′	0
TFO3AA	3′ **AGGGAGAGGGGAAGAGA** 5′	0
TFO3B	3′ **TGGGTGTGGGGTTGTGT**TC 5′	2
TFO3C	3′ **AGGGAGAGGGGAAGAGA**TC 5′	2
TFO3D	3′ **TGGGTGTGGGGTTGTGT**CTT 5′	4
TFO3E	3′ **AGGGAGAGGGGAAGAGA**TCTA 5′	4
TFO3F	3′ **TGGGTGTGGGGTTGTGT**CTTCT 5′	6
TFO3G	3′ **AGGGAGAGGGGAAGAGA**TCTACT 5′	6
TFO3H	3′ **TGGGTGTGGGGTTGTGT**CTTCTCT 5′	8
TFO3I	3′ **AGGGAGAGGGGAAGAGA**TCTACTCA 5′	8
TFO3J	3′ **TGGGTGTGGGGTTGTGT**CTTCTCTGG 5′	10
TFO3K	3′ **AGGGAGAGGGGAAGAGA**TCTACTCAGG 5′	10
TFO3L	3′ **TGGGTGTGGGGTTGTGT**CT 5′	2
TFO3M	3′ **AGGGAGAGGGGAAGAGA**CT 5′	2
TFO3N	3′ **TGGGTGTGGGGTTGTGT**CTCG 5′	4
TFO3O	3′ **AGGGAGAGGGGAAGAGA**CTCG 5′	4
TFO3P	3′ **TGGGTGTGGGGTTGTGT**CTCGTT 5′	6
TFO3Q	3′ **AGGGAGAGGGGAAGAGA**CTCGTT 5′	6
TFO3R	3′ **AGGGAGAGGGGAAGTGT**CTCGTT 5′	6
TFO3S	3′ **AGGGAGAGGGGTTGTGT**CTCGTT 5′	6
TFO3T	3′ **TGGGTGTGGGGTTGTGT**CTCGTTTG 5′	8
TFO3U	3′ **AGGGAGAGGGGAAGAGA**CTCGTTTG 5′	8
TFO3V	3′ **TGGGTGTGGGGTTGTGT**CTCGTTTGTC 5′	10
TFO3W	3′ **AGGGAGAGGGGAAGAGA**CTCGTTTGTC 5′	10

[a] The target duplex is shown in boldface in the first row. Flanking DNA corresponding to rhodopsin genomic sequence is shown in regular type in the first line. TFO sequences are shown in boldface type with linker nucleotides in regular type. The orientation of the TFO is shown relative to the purine-rich strand of the target duplex. [b] Numbers refer to the number of linker nucleotides in the TFO.

TFO binding affinities were estimated by electrophoretic mobility shift assays (band shift assays) as previously described (*35*, *36*), and the results are shown in Figure 1. As observed previously (*35*), the GA−TFO conjugates bound with a 10-fold higher affinity than the corresponding GT−TFO conjugates. The binding of GA−TFO conjugates with antiparallel linkers was relatively insensitive to linker length, decreasing only about 3-fold for 10 extra nucleotides (Figure 1A). GT−TFO conjugates with antiparallel linkers experienced decreases in binding affinity of a similar extent (Figure 1A). Binding by GA−TFO conjugates with alternate-strand linkers was also only moderately affected by linker nucleotides (Figure 1B). However, GT−TFO conjugates designed with alternate-strand linkers were very sensitive to linker length; even four additional nucleotides reduced the binding affinity by 100-fold (Figure 1B; TFO3N). On the basis of these results, the linkers on all TFOs used in subsequent experiments were designed using the standard rules for triplex formation.

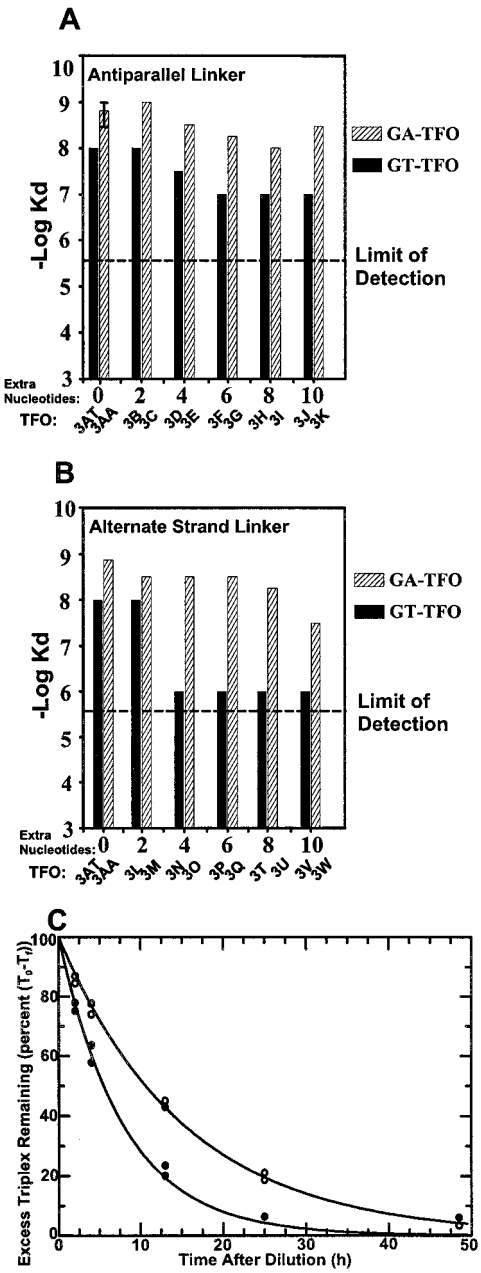

FIGURE 1: Effects of linkers on TFO binding affinities and dissociation kinetics. (A) Linkers designed to bind using antiparallel, purine motif rules of triplex formation. (B) Linkers designed to bind in an alternate-strand manner, using parallel, pyrimidine motif rules. Binding affinities were determined by band shift analysis using synthetic duplexes. The negative logarithm of the estimated dissociation constant is plotted, with the error bar for TFO3AA representing the range of values obtained in multiple independent assays over a period of several months, to illustrate the uncertainty in the estimates. Black bars represent data for GT−TFO conjugates; hatched bars represent data for GA−TFO conjugates. The dotted line represents the limit of detection for this assay. TFO3R and TFO3S, whose binding was too weak to be detected, were not plotted in these figures. (C) Dissociation of triplexes formed by TFO3AA (no linker) and TFO3K (10-nucleotide linker). The fraction of total labeled duplex in triplex form is plotted as a function of time following dilution. Raw data were fit to the equation $T(t) = T_f + (T_0 - T_f) \exp(-k_{eff}t)$, where $T(t)$ is the fraction total duplex in triplex form at time t. The points are plotted on a percentage scale relative to $T_0 - T_f$, with 100% corresponding to T_0 and 0% corresponding to T_f. The best fit values were as follows: $T_0 = 0.843$, $T_f = 0.596$, and $k_{eff} = 1.76 \times 10^{-5}$ s^{-1} for TFO3AA and $T_0 = 0.784$, $T_f = 0.527$, and $k_{eff} = 3.5 \times 10^{-5}$ s^{-1} for TFO3K. The first-order rate constants were calculated form the equation $k_1 = k_{eff}(1 - T_f)$.

Effect of Linkers on TFO Binding Kinetics. Dissociation kinetics for GA−TFO conjugates with and without antiparallel linkers were compared and found to differ by about the same magnitude as the differences in their binding affinities. TFO3K, which has a 10-nucleotide linker, dissociated from the triplex with a first-order rate constant, k_1 (*36*), of 1.66×10^{-5} s^{-1}, about 2-fold faster than TFO3AA, which has no extra nucleotides and dissociated with a k_1 of 0.71×10^{-5} s^{-1} (Figure 1C).

Footprint Analysis of Linker TFOs. Although the nucleotides in the linker region of the TFO were designed according to standard antiparallel triplex rules, they were not expected to bind tightly to the underlying duplex because the TFO strand contained many pyrimidine bases, which interact only very weakly, if at all, with the purine-rich strand of the duplex. To assess whether triplex formation occurred in the linker region, we used DNase I footprinting since regions of a duplex that form triplexes are protected from DNase I cleavage (*44*, *45*). If nucleotides in the linker were participating in a triplex, the footprint would extend beyond the core footprint produced by a TFO with no additional nucleotides (Figure 2A, lane 3, TFO3AA). GT− and GA− TFO conjugates with various linker lengths were incubated with a target duplex that had only the purine-rich strand labeled. TFOs were used at a high concentration (10^{-6} M) to permit triplex formation and at a low concentration (10^{-10} M), which is below the K_d for triplex formation. Regardless of linker length, at the high concentration all TFOs protected the same core region of the duplex (Figure 2). In no case did a linker extend the footprint (toward the top of the gel), as would be expected if linker nucleotides were involved in a triplex. In addition, as is characteristic of triplex formation, a DNase I-hypersensitive site was induced adjacent to the core footprint (Figure 2, arrow) in the absence of linker nucleotides (lane 3). The same hypersensitive site is present in all footprints, regardless of linker length. The absence of an extended footprint and the unchanging position of the hypersensitive site indicate that the linker nucleotides do not form a sufficiently stable interaction with the underlying duplex to protect it from DNase I digestion.

Photoadduct Formation at the Triplex−Duplex Junction. As a basis for comparing the efficiency of linkers in promoting psoralen cross-linking at distant sites, we first assessed psoralen photoadduct (cross-link and monoadduct) formation at duplex 2 and duplex 9, which contain a 5′-ApT at the boundary of duplex and triplex DNA (Table 1). GA−TFO conjugates with psoralen attached to their 5′-ends were synthesized to bind the synthetic duplexes (Figure 3A). In agreement with previous results (*46*), psoralen did not enhance the binding affinity of the TFO (data not shown). Psoralen−TFO conjugates were incubated at a high concentration (10^{-6} M) with target duplexes under conditions which were suitable for triplex formation. The triplexes were irradiated with ultraviolet (UVA) light, and monoadducts and cross-links were efficiently formed (Figure 3B). Quantitation of radioactive products by PhosphorImage analysis indicated that photoadduct formation occurred with first-order reaction kinetics (data not shown) and was complete after 60 min. PhosphorImage analysis also indicated a total photoadduct yield of 77% (±1.2%) after 60 min, with cross-links comprising 65% (±1.1%) of the total radioactivity with duplex 2 (Figure 3B, lanes 9 and 10). Duplex 9 also gave a

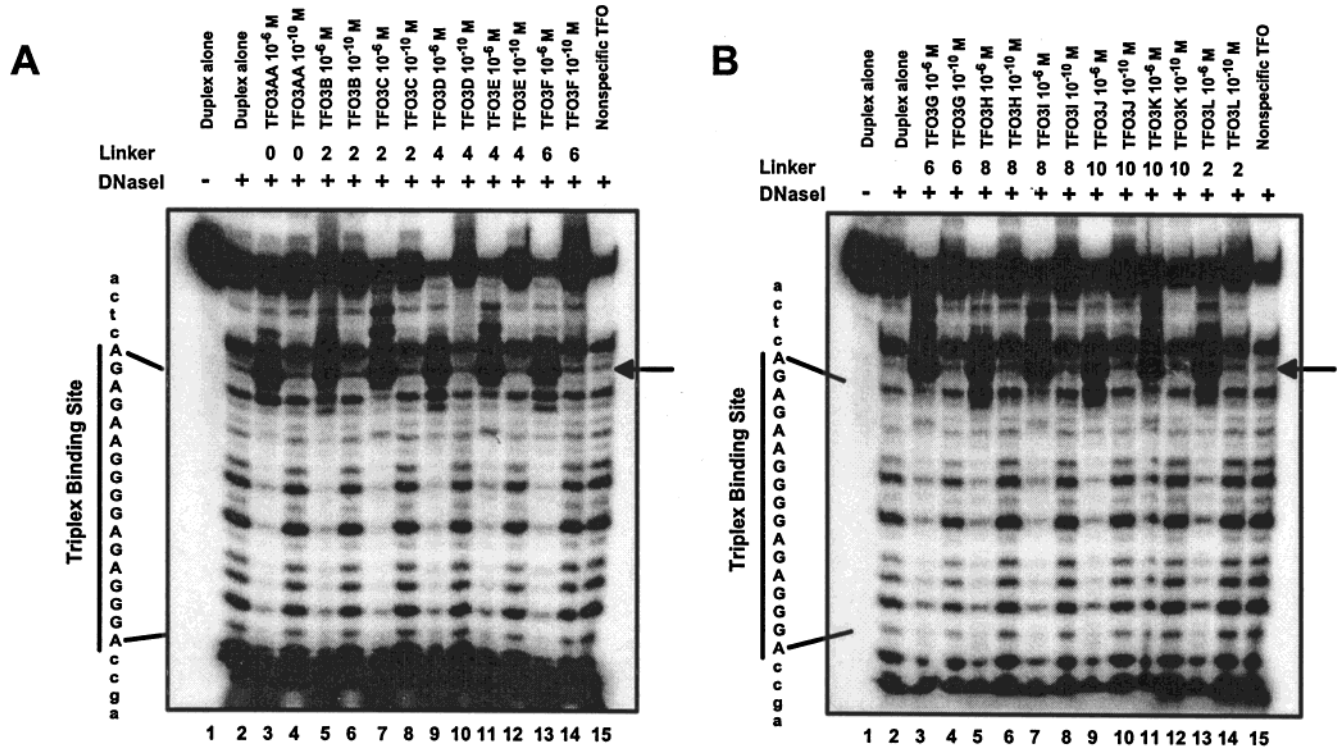

FIGURE 2: DNase I protection analysis of triplex formation. Duplex 3 was 5′-end-labeled on the purine-rich strand and assayed for DNase I protection by various TFOs. Reaction products were separated by denaturing PAGE on 15% gels and analyzed by autoradiography. The expected triplex binding site was identified from DMS and piperidine treatment of the duplex to indicate the G nucleotides in the sequence (data not shown). The arrow indicates the DNase I hypersensitive site present at the triplex−duplex junction. Nonspecific TFO refers to a TFO that does not form a triplex with this duplex: (A) TFO3AA−TFO3F and (B) TFO3G−TFO3L.

Table 3: Target Duplexes and Psoralen−TFO Conjugates with Linkers

Target or TFO	Sequence[a]	Linker Length[b]
Duplex 3	5′ AAACTGAGGC**AGGGAGAGGGGAAGAGA**CTCATTTAGG 3′ 3′ TTTGACTCCG**TCCCTCTCCCCTTCTCT**GAGTAAATCC 5′	
Duplex 3A	5′ AAACTGAGGC**AGGGAGAGGGGAAGAGA**CTCTTTTAGG 3′ 3′ TTTGACTCCG**TCCCTCTCCCCTTCTCT**GAGAAAATCC 5′	
Duplex 3B	5′ AAACTGAGGC**AGGGAGAGGGGAAGAGA**CTCATTTTGG 3′ 3′ TTTGACTCCG**TCCCTCTCCCCTTCTCT**GAGTAAAACC 5′	
Duplex 3C	5′ AAACTGAGGC**AGGGAGAGGGGAAGAGA**CTCGTTTAGG 3′ 3′ TTTGACTCCG**TCCCTCTCCCCTTCTCT**GAGCAAATCC 5′	
psorTFO31	3′ **AGGGAGAGGGGAAGAGA**TC-P 5′	2
psorTFO32	3′ **AGGGAGAGGGGAAGAGA**TCT-P 5′	3
psorTFO33	3′ **AGGGAGAGGGGAAGAGA**TCTA-P 5′	4
psorTFO34	3′ **AGGGAGAGGGGAAGAGA**TCTAC-P 5′	5
psorTFO35	3′ **AGGGAGAGGGGAAGAGA**TCTACT-P 5′	6
psorTFO36	3′ **AGGGAGAGGGGAAGAGA**TCTACTC-P 5′	7
psorTFO37	3′ **AGGGAGAGGGGAAGAGA**TCTACTCA-P 5′	8
psorTFO38	3′ **AGGGAGAGGGGAAGAGA**TCTACTCAG-P 5′	9
PsorTFO39	3′ **AGGGAGAGGGGAAGAGA**TCTGCTCA-P 5′	8

[a] The target duplexes are shown in boldface in the first box. Flanking DNA is shown in regular type in the first line. Potential psoralen cross-linking sites are underlined. TFO sequences are shown in boldface type in subsequent boxes with linker nucleotides in regular type. P stands for psoralen. The orientation of the TFO is shown relative to the purine-rich strand of the target duplex. [b] Numbers refer to the number of linker nucleotides in the TFO.

high yield of total photoadducts (70 ± 2.2%) with cross-links being 56% (±1.6%) of the total radioactivity (Figure 3B, lanes 15 and 16).

Photoadduct Formation at Sites Distant from the Triplex−Duplex Junction. To measure the efficiency of linker-mediated cross-linking at distant sites, we chose to use duplex 3, which has two potential psoralen cross-linking sites, four and seven nucleotides from the triplex−duplex junction (Table 3 and Figure 4A). TFOs were designed to have a psoralen attached to linkers of increasing length, from two to nine nucleotides (Table 3). When these TFOs were incubated at a high concentration (10^{-6} M) with the duplex and irradiated with UVA light, monoadducts and cross-links were formed as shown for linker lengths of four and five nucleotides in Figure 4B. As is apparent, there are more species of monoadduct present in Figure 4 than in Figure 3. We attribute this increased heterogeneity, which is generally observed for TFOs with linkers, to the increased opportunity for reaction at more distant sites. Labeling of individual strands of the duplex reveals that monoadduct species are uniquely associated with one strand or the other (data not shown), as expected, but we have not characterized them further.

Cross-link formation was essentially complete after UVA irradiation for 60 min, regardless of the linker length (Figure 5A). As shown in Figure 5A, the cross-linking efficiency reached a maximum (∼25%) when the psoralen was extended to the 5′-ApT site four nucleotides from the triplex junction. A low level (∼5%) of cross-linking occurred with psoralen−TFO conjugates having seven-, eight-, or nine-nucleotide linkers (Figure 5A). These TFOs may have formed cross-links at the 5′-TpA site, or the linkers may have been sufficiently flexible to cross-link the 5′-ApT site.

To determine whether cross-linking occurred at the 5′-ApT site, the 5′-TpA site, or both, two additional duplexes were synthesized (Table 3). In duplex 3A, the 5′-ApT site was abolished by inverting the A·T base pair, which created a 5′-TpT site. In duplex 3B, the 5′-TpA site was removed by inverting the A·T base pair, creating a 5′-TpT site. Psoralen-conjugated TFOs were incubated at high concentra-

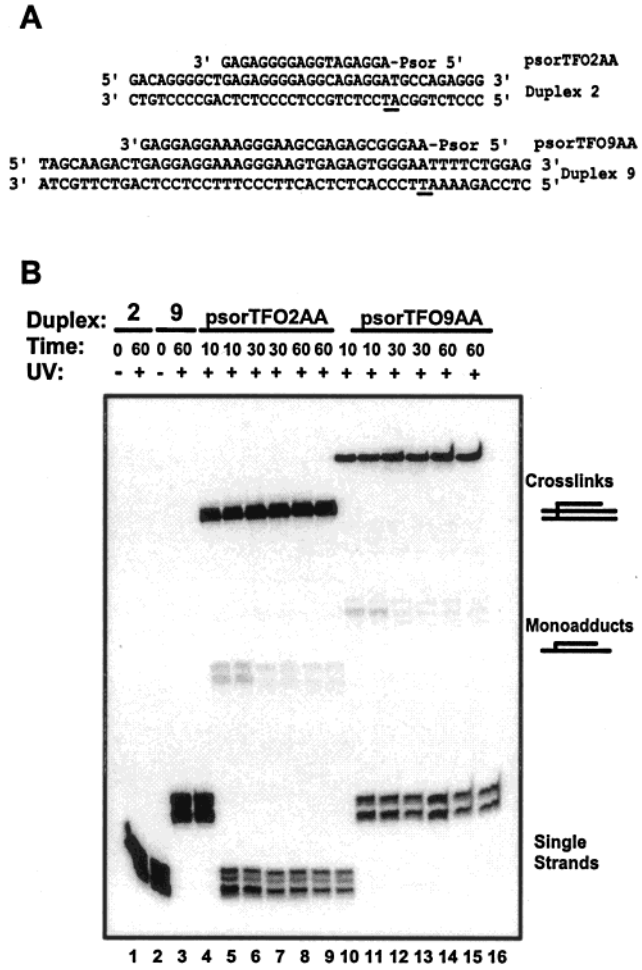

FIGURE 3: Electrophoretic analysis of photoadducts formed at psoralen cross-linking sites located at the triplex junction. (A) Target duplexes and psoralen−TFO conjugates used in this assay. The expected psoralen cross-linking site in each duplex is underlined. (B) Photoadducts formed by psoralen cross-linking. End-labeled target duplexes were incubated with psoralen−TFO conjugates for 24 h and irradiated with UV light for the indicated periods of time. Products were separated by denaturing PAGE on 15% gels and analyzed by autoradiography. Migration positions on the gel are indicated for the duplex single strands, monoadducts (two connected lines), and cross-links (three connected lines).

tions with these duplexes to form a triplex, and irradiated with UVA light. In duplex 3B, cross-links still formed with modest efficiency (∼17%) with a four-nucleotide linker TFO, but cross-links were formed with a lower efficiency (<3%) using an eight-nucleotide linker TFO (Figure 5B, dotted line). These results strongly suggest that the cross-links formed with the four-nucleotide linker TFO occurred at the 5′-ApT and not the more distant 5′-TpA. In duplex 3A, only a minimal amount of cross-links formed (<2%) with a four-nucleotide linker; however, no cross-links (<1%) were formed with an eight-nucleotide linker (Figure 5B, □). These results indicate that the 5′-ApT is the principal site for cross-links and that the more distant 5′-TpA site is rarely, if ever, cross-linked.

The yield of total photoadducts for all duplexes with psoralen-preferred sites beyond the junction was highest (30−44%) with two- to four-nucleotides linkers, and decreased with increasing length, except for duplex 3, where the total amount of photoadducts increased for TFOs having eight- and nine-nucleotide linkers (Figure 5D). To test

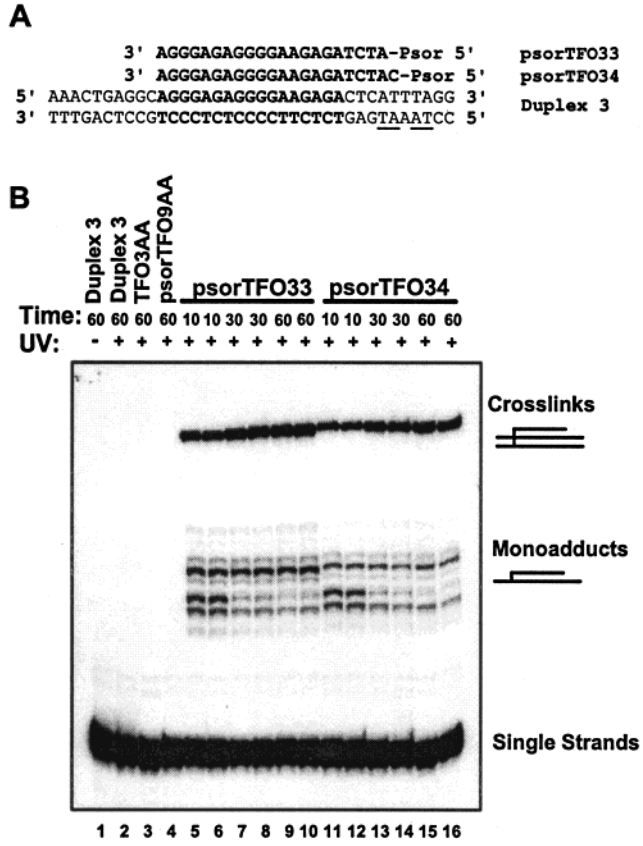

FIGURE 4: Electrophoretic analysis of photoadducts formed at psoralen cross-linking sites located away from the triplex junction. (A) Target duplex and psoralen−TFO conjugates with linker lengths of four (psorTFO33) and five (psorTFO34) nucleotides. The triplex binding site is shown in boldface. The potential psoralen cross-linking sites are underlined in the target duplex. (B) Representative experiment of photoadduct formation by psoralen−TFO conjugates with linkers. The experiment was performed as described in the legend of Figure 3B.

whether transient triplet formation at the A four nucleotides away from the triplex junction in duplex 3 (Table 3) might be responsible for this enhancement, we designed duplex 3C, which carries a G at that position, and the corresponding eight-nucleotide linker TFO with a G four nucleotides away from the triplex junction (Table 3, psorTFO39). We reasoned that if transient triplet formation at that position was responsible for an increased level of monoadducts, psorTFO39 should react with duplex 3C much like psorTFO37 reacts with duplex 3. However, psorTFO39 should react poorly with duplex 3, and psorTFO37 should react poorly with duplex 3C. Contrary to these expectations, psorTFO37 and psorTFO39 formed a similar high level of monoadducts with both duplexes (data not shown), arguing against a contribution of triplex formation by the linker.

The general decrease in the extent of photoadduct formation with longer linkers (Figure 5D) could arise, in principle, from a psoralen-mediated increased tendency toward self-association and self-reaction of TFOs with longer linkers. To test this possibility, the psoralen-modified GA−TFO conjugates with various linker lengths were 3′-end-labeled, incubated under triplex-forming conditions in the absence of duplex, UVA irradiated, and analyzed by electrophoresis on denaturing polyacrylamide gels. Significant self-reaction, as revealed by a slower migrating species, was observed for all TFOs at a high concentration (10^{-6} M), but not at a low

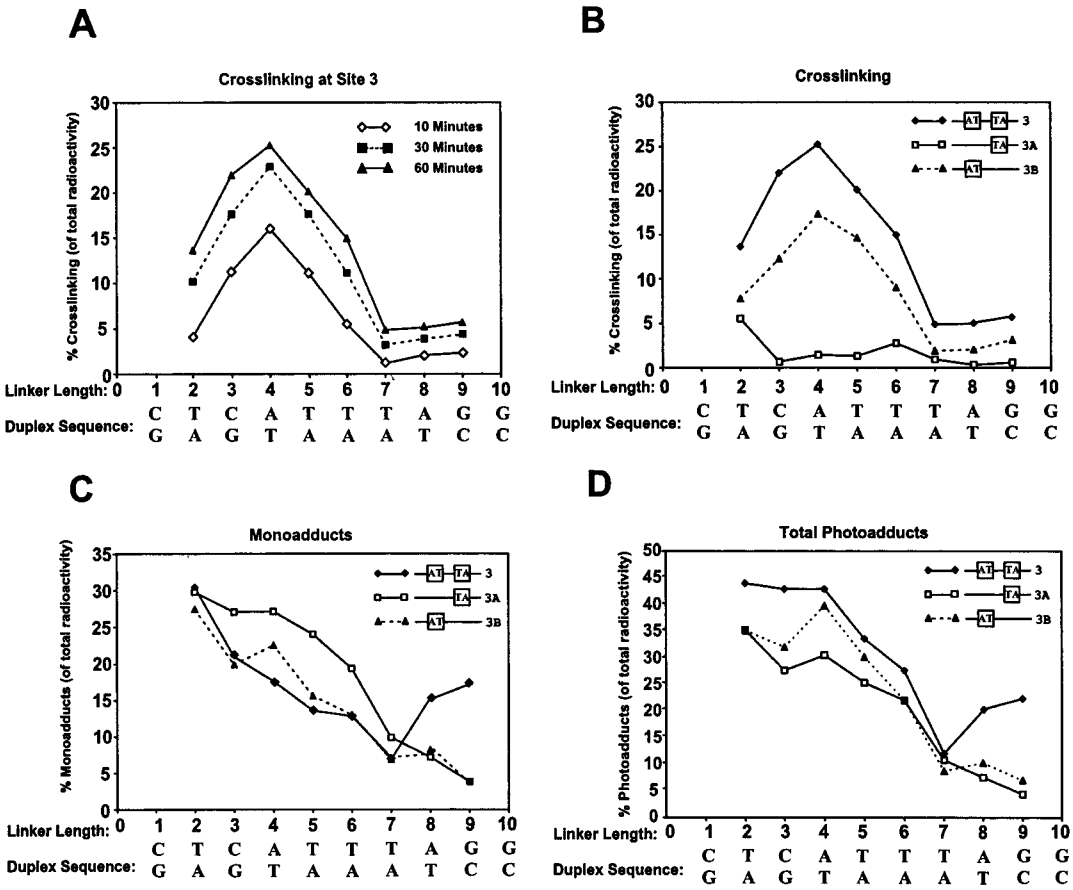

FIGURE 5: Kinetics and photoproduct distribution of psoralen−TFO conjugates with nucleotide linkers. (A) Time course of cross-link formation at duplex 3. Radioactivity from cross-link species identified by mobility (Figure 4B) was quantified using a PhosphorImager and plotted as a percent of total radioactivity vs the linker length of each TFO. The extent of cross-link formation increased from 10 min of UVA irradiation (◇) to UVA irradiation for 30 min (■) and was nearly complete by 60 min (▲). In panels B−D are shown photoadducts formed with three different duplexes after irradiation for 60 min. Black diamonds represent data for duplex 3, white squares data for duplex 3A, and black triangles data for duplex 3B. The amounts of cross-links (B), monoadducts (C), or total photoadducts (cross-links and monoadducts, D) were plotted as a function of linker length.

concentration (10^{-10} M), indicating that the association was intermolecular (data not shown). At 10^{-6} M TFO, the level of self-reaction was highest for TFOs with short linkers (55, 60, and 42% for TFOs with two-, three-, and four-nucleotide linkers, respectively) and lowest for TFOs with long linkers (9, 9, and 10% for TFOs with seven-, eight-, and nine-nucleotide linkers, respectively). These results are the opposite of those expected if self-association were the explanation for the decrease in the level of photoadduct formation observed in Figure 5D. Moreover, when the labeled TFOs were incubated with an excess of target duplex, TFO self-reaction was abolished (data not shown), indicating that triplex formation competes effectively with self-association. These results rule out TFO self-association as an explanation for a decreased extent of photoadduct formation with increasing linker length.

Reactivity of Psoralen−TFO Conjugates at 5′-TpA and 5′-ApT Sequences. Although free psoralen cross-links 5′-TpA sites at least 10-fold more efficiently than 5′-ApT sites (*29*, *30*, *32*, *47*, *48*), both sites have been used successfully as targets for cross-linking by psoralen tethered to TFOs (*49*, *50*). The reactivity of psoralen−TFO conjugates, however, has not been directly compared at 5′-TpA and 5′-ApT in identical sequence contexts. To measure relative reactivity, we modified duplex 3 to contain either a 5′-TpA (duplex 3TA) or a 5′-ApT (duplex 3AT) two nucleotides away from the triplex junction (Figure 6A). A psoralen−TFO conjugate with a two-nucleotide linker was incubated with both duplexes; the triplexes were subsequently irradiated with UVA light, and the photoadducts were analyzed (Figure 6B). Quantitation of the photoadducts showed that the 5′-TpA sequence formed cross-links with moderately higher efficiency (56%) than the 5′-ApT sequence (38%), although the total amounts of photoadducts were comparable (Figure 6C). These results indicate that 5′-TpA and 5′-ApT are roughly equivalent targets for psoralen when it is tethered to a TFO.

DISCUSSION

Formation of triplex DNA provides a potential method for targeting DNA-damaging agents to defined sites in specific genes, as a way of modifying their expression or altering their sequence. Previously, we identified and characterized multiple triplex sites in the human rhodopsin gene as an initial step in developing triplex technology as a treatment for the disease ADRP (*35*). Here, we have extended those studies to examining the usefulness of psoralen−TFO conjugates for introducing site-specific damage adjacent to triplex targets in the rhodopsin gene. As discussed in detail previously (*35*), triplex-mediated, rhodopsin-specific gene damage could serve as a plausible therapy for ADRP by sensitizing the locus to correction by homologous recombi-

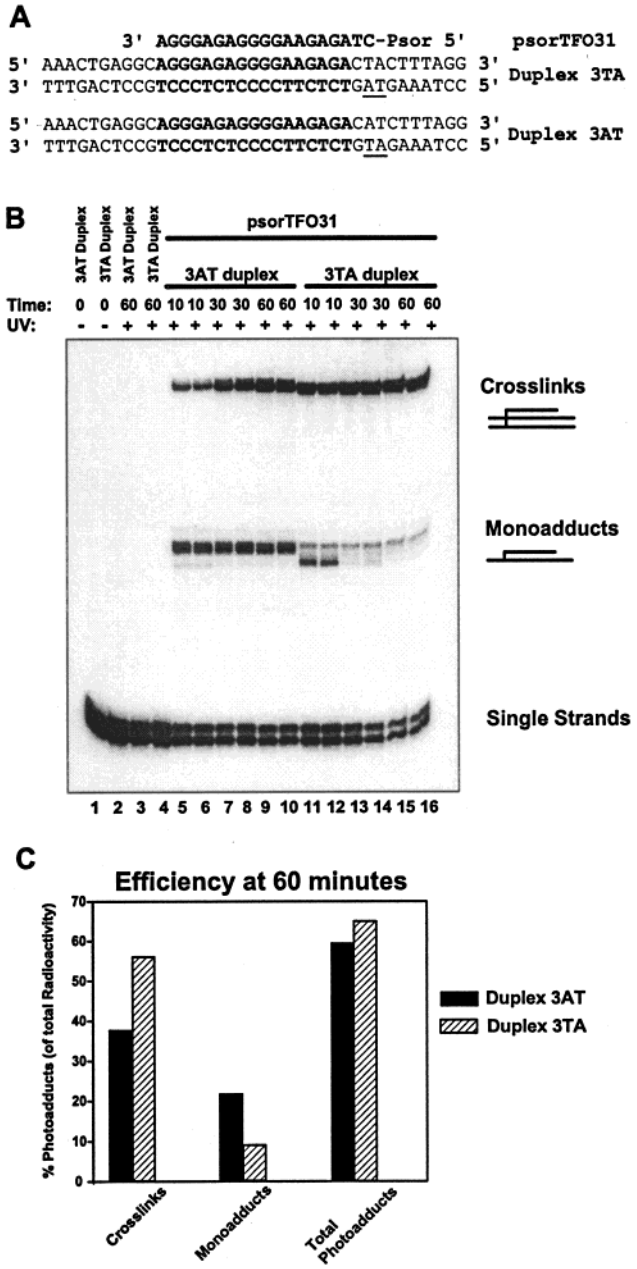

FIGURE 6: Comparison of photoadduct formation at 5′-ApT or 5′-TpA sites. (A) Target duplexes and psoralen−TFO conjugates used in these assays. The target binding site is shown in boldface, and the potential cross-linking site is underlined in the duplex. (B) Autoradiogram showing photoadduct formation with psoralen−TFO conjugates. Experiments were performed as described in the legend of Figure 3B. (C) The radioactivity from cross-links, monoadducts, and the total photoadducts after 60 min was plotted as a percentage of total radioactivity for target duplexes with either a 5′-ApT site (black bars) or a 5′-TpA site (hatched bars).

nation or by interfering with gene expression by blocking transcription.

Distribution of Psoralen-Reactive Sites around Triplex Targets. Psoralens are a class of photoactivatable DNA-damaging agents that have proven to be especially useful in cellular experiments because they are innocuous until exposed to UVA irradiation at wavelengths that are minimally harmful to cellular constituents. In addition, psoralen can cross-link the two DNA strands, which can effectively block transcription by RNA polymerase (*51*) and substantially stimulate homologous recombination (*52*). Previous reports (*29*, *30*, *32*, *47*, *48*) indicate that free psoralen preferentially cross-links 5′-TpA and 5′-ApT sites, with 5′-TpA sites favored by at least 10-fold. Most studies using psoralen-conjugated TFOs have targeted 5′-TpA sites located at the duplex−triplex junction or immediately adjacent to it and have demonstrated cross-linking efficiencies approaching 100% (*50*, *53*−*55*), but more typically in the range of 25−80% (*46*, *56*−*59*). In this study, two 5′-ApT sites at the junction were cross-linked with efficiencies of 56 and 65% (Figure 3). In addition, in a direct comparison of the relative reactivity of 5′-TpA and 5′-ApT in the identical sequence context two nucleotides away from the junction, we showed that cross-linking at 5′-TpA sites (56%) was only moderately more efficient than at 5′-ApT sites (38%). Thus, in contrast to the results with free psoralen, 5′-TpA and 5′-ApT are roughly equivalent targets for cross-linking by psoralen tethered to a TFO.

Our goal in using nucleotide linkers to position psoralen for photoreaction at 5′-TpA and 5′-ApT sites more distant from the junction was to increase the number of triplex targets that are amenable to psoralen cross-linking. As discussed below, nucleotide linkers were reasonably effective at promoting cross-linking at a 5′-ApT site located four and five nucleotides from a triplex−duplex junction. What fraction of triplex targets would be expected to have a 5′-TpA or a 5′-ApT within five nucleotides of a junction? On a statistical basis, it can be shown that about 45% of purine runs (potential triplex targets) should have a psoralen target at a junction and about 80% should have a psoralen target within five nucleotides. Of the 17 long purine runs that we identified and tested for triplex formation in the human rhodopsin gene (*35*), five (29%) have a psoralen target at a junction and an additional seven (71%) have a psoralen target with five nucleotides. These targets occur at both the 5′- and 3′-sides of the purine-rich strand of the target. Thus, the use of nucleotide linkers to tether psoralen should approximately double the number of triplex targets that are available for psoralen cross-linking.

Utility of Nucleotide Linkers in Tethering Psoralen to TFOs. In previous studies, we demonstrated that psoralen tethered by a standard six-carbon linker was ineffective at cross-linking 5′-TpA sites more than one nucleotide away from a duplex−triplex junction (*46*). Psoralens tethered by longer carbon linkers (up to 86 carbons in length) have been tested for their ability to cause mutations in the *supFG1* gene in an SV40-based shuttle vector (*39*). Perhaps due to the hydrophobic and flexible nature of this carbon linker, the intercalation position of the psoralen varied and the subsequent cross-linking and mutation frequencies were low.

To test a more rigid and hydrophilic linker structure, we attached a psoralen molecule to the TFO via additional nucleotides. Linker−TFO conjugates that did not have psoralen exhibited a modest decrease in binding affinity with increasing linker length, although the decrease was only about 3-fold for linkers up to 10 nucleotides long (Figure 1). It is possible that at a sufficient length, the linker nucleotides will prohibit TFO binding, which limits the distance from the triplex junction where a TFO can still cause DNA damage.

Psoralen−TFO conjugates with specific linker lengths mediated cross-link formation with good efficiency (25%) and site specificity at short distances, four nucleotides, from

the triplex junction. However, at longer distances from the triplex junction (7−10 bp), the yield of cross-links was low. This decrease is likely due to the increased level of electrostatic repulsion between the negative charge on the nucleotide linker and the negative charge on the duplex as well as to unfavorable entropic effects incurred by a long linker. The overall cross-linking efficiencies (25%) and photoadduct yields (45%) from a four-nucleotide linker (Figure 5A) suggest that unmodified nucleotide linkers are a reasonable method of causing targeted DNA damage at 5′-ApT and 5′-TpA sites within five nucleotides of the triplex junction. Modified oligonucleotides with neutral (*60*) or positively charged backbones (*61*) may provide the additional stability required for high photoadduct yields at more distant sites.

Utility of Multiple Psoralen Target Sites. We have demonstrated triplex-mediated DNA psoralen cross-linking at three sites in the human rhodopsin gene. In our previous study (*35*), we demonstrated that long homopurine sequences, which are ideal for triplex formation, are more abundant than expected in human genes. The ability to target damage to multiple sites increases the likelihood of obtaining the desired effect. Using a plasmid based reporter assay, in which TFOs are reacted with a plasmid in vitro and then transfected into cells, we have shown that rhodopsin expression is inhibited by 70−75% after reaction with either psoralen−TFO2 or psoralen−TFO9, but is decreased by 90% when the two TFOs are combined (unpublished data). Intracellular potassium concentrations (*36*), nucleosomes (*62*, *63*), and nucleases are all challenges for triplex formation inside the cell. Modified backbones and nucleotides (*64*−*69*) can minimize the effects of potassium and nucleases, and recent in vitro evidence suggests that a triplex can be formed on the nucleosome, dependent upon target site positioning within the core (*70*). We are now testing the DNA damaging effects of single and multiple TFOs on transcription inhibition, homologous recombination, and mutation induction on mammalian chromosomes in tissue culture.

REFERENCES

1. Nathans, J. (1992) *Biochemistry 31*, 4923−4931.
2. Rao, V. R., and Oprian, D. D. (1996) *Annu. Rev. Biophys. Biomol. Struct. 25*, 287−314.
3. Berson, E. L. (1996) *Proc. Natl. Acad. Sci. U.S.A. 93*, 4526−4528.
4. Heckenlively, J. R. (1988) *Retinitis Pigmentosa*, J. B. Lippincott, Philadelphia.
5. Humphries, M. M., Rancourt, D., Farrar, G. J., Kenna, P., Hazel, M., Bush, R. A., Sieving, P. A., Sheils, D. M., McNally, N., Creighton, P., Erven, A., Boros, A., Gulya, K., Capecchi, M. R., and Humphries, P. (1997) *Nat. Genet. 15*, 216−219.
6. Rosenfeld, P. J., Cowley, G. S., McGee, T. L., Sandberg, M. A., Berson, E. L., and Dryja, T. P. (1992) *Nat. Genet. 1*, 209−213.
7. Vasquez, K. M., and Wilson, J. H. (1998) *Trends Biochem. Sci. 23*, 4−9.
8. Ing, N. H., Beekman, J. M., Kessler, D. J., Murphy, M., Jayaraman, K., Zendegui, J. G., Hogan, M. E., O'Malley, B. W., and Tsai, M. J. (1993) *Nucleic Acids Res. 21*, 2789−2796.
9. Kovacs, A., Kandala, J. C., Weber, K. T., and Guntaka, R. V. (1996) *J. Biol. Chem. 271*, 1805−1812.
10. Svinarchuk, F., Debin, A., Bertrand, J. R., and Malvy, C. (1996) *Nucleic Acids Res. 24*, 295−302.
11. Kochetkova, M., and Shannon, M. F. (1996) *J. Biol. Chem. 271*, 14438−14444.
12. Orson, F. M., Thomas, D. W., McShan, W. M., Kessler, D. J., and Hogan, M. E. (1991) *Nucleic Acids Res. 19*, 3435−3441.
13. Postel, E. H., Flint, S. J., Kessler, D. J., and Hogan, M. E. (1991) *Proc. Natl. Acad. Sci. U.S.A. 88*, 8227−8231.
14. McShan, W. M., Rossen, R. D., Laughter, A. H., Trial, J., Kessler, D. J., Zendegui, J. G., Hogan, M. E., and Orson, F. M. (1992) *J. Biol. Chem. 267*, 5712−5721.
15. Scaggiante, B., Morassutti, C., Tolazzi, G., Michelutti, A., Baccarani, M., and Quadrifoglio, F. (1994) *FEBS Lett. 352*, 380−384.
16. Okada, T., Yamaguchi, K., and Yamashita, Y. (1994) *Growth Factors 11*, 259−270.
17. Thomas, T. J., Faaland, C. A., Gallo, M. A., and Thomas, T. (1995) *Nucleic Acids Res. 23*, 3594−3599.
18. Tu, G. C., Cao, Q. N., and Israel, Y. (1995) *J. Biol. Chem. 270*, 28402−28407.
19. Porumb, H., Gousset, H., Letellier, R., Salle, V., Briane, D., Vassy, J., Amor-Gueret, M., Israel, L., and Taillandier, E. (1996) *Cancer Res. 56*, 515−522.
20. Rininsland, F., Johnson, T. R., Chernicky, C. L., Schulze, E., Burfeind, P., Ilan, J., and Ilan, J. (1997) *Proc. Natl. Acad. Sci. U.S.A. 94*, 5854−5859.
21. Aggarwal, B. B., Schwarz, L., Hogan, M. E., and Rando, R. F. (1996) *Cancer Res. 56*, 5156−5164.
22. Sandor, Z., and Bredberg, A. (1994) *Nucleic Acids Res. 22*, 2051−2056.
23. Wang, G., Levy, D. D., Seidman, M. M., and Glazer, P. M. (1995) *Mol. Cell. Biol. 15*, 1759−1768.
24. Wang, G., Seidman, M. M., and Glazer, P. M. (1996) *Science 271*, 802−805.
25. Majumdar, A., Khorlin, A., Dyatkina, N., Lin, F. L., Powell, J., Liu, J., Fei, Z., Khripine, Y., Watanabe, K. A., George, J., Glazer, P. M., and Seidman, M. M. (1998) *Nat. Genet. 20*, 212−214.
26. Faruqi, A. F., Seidman, M. M., Segal, D. J., Carroll, D., and Glazer, P. M. (1996) *Mol. Cell. Biol. 16*, 6820−6828.
27. Sandor, Z., and Bredberg, A. (1995) *Biochim. Biophys. Acta 1263*, 235−240.
28. Cimino, G. D., Gamper, H. B., Isaacs, S. T., and Hearst, J. E. (1985) *Annu. Rev. Biochem. 54*, 1151−1193.
29. Esposito, F., Brankamp, R. G., and Sinden, R. R. (1988) *J. Biol. Chem. 263*, 11466−11472.
30. Boyer, V., Moustacchi, E., and Sage, E. (1988) *Biochemistry 27*, 3011−3018.
31. Gia, O., Magno, S. M., Garbesi, A., Colonna, F. P., and Palumbo, M. (1992) *Biochemistry 31*, 11818−11822.
32. Sage, E., and Moustacchi, E. (1987) *Biochemistry 26*, 3307−3314.
33. Rouet, P., Smih, F., and Jasin, M. (1994) *Mol. Cell. Biol. 14*, 8096−8106.
34. Sargent, R. G., Brenneman, M. A., and Wilson, J. H. (1997) *Mol. Cell. Biol. 17*, 267−277.
35. Perkins, B. D., Wilson, J. H., Wensel, T. G., and Vasquez, K. M. (1998) *Biochemistry 37*, 11315−11322.
36. Vasquez, K. M., Wensel, T. G., Hogan, M. E., and Wilson, J. H. (1995) *Biochemistry 34*, 7243−7251.
37. Xodo, L. E., Pirulli, D., and Quadrifoglio, F. (1997) *Eur. J. Biochem. 248*, 424−432.
38. Sambrook, J., Fritsch, E. F., and Maniatis, T. (1989) *Molecular Cloning: A Laboratory Manual*, Cold Spring Harbor Laboratory Press, Cold Spring Habor, NY.
39. Raha, M., Lacroix, L., and Glazer, P. M. (1998) *Photochem. Photobiol. 67*, 289−294.
40. Chandler, S. P., and Fox, K. R. (1996) *Biochemistry 35*, 15038−15048.
41. Jayasena, S. D., and Johnston, B. H. (1992) *Nucleic Acids Res. 20*, 5279−5288.
42. de Bizemont, T., Duval-Valentin, G., Sun, J. S., Bisagni, E., Garestier, T., and Helene, C. (1996) *Nucleic Acids Res. 24*, 1136−1143.
43. Washbrook, E., and Fox, K. R. (1994) *Nucleic Acids Res. 22*, 3977−3982.

44. Cassidy, S. A., Strekowski, L., Wilson, W. D., and Fox, K. R. (1994) *Biochemistry 33*, 15338−15347.
45. Brown, P. M., Drabble, A., and Fox, K. R. (1996) *Biochem. J. 314*, 427−432.
46. Vasquez, K. M., Wensel, T. G., Hogan, M. E., and Wilson, J. H. (1996) *Biochemistry 35*, 10712−10719.
47. Zhen, W. P., Buchardt, O., Nielsen, H., and Nielsen, P. E. (1986) *Biochemistry 25*, 6598−6603.
48. Gamper, H., Piette, J., and Hearst, J. E. (1984) *Photochem. Photobiol. 40*, 29−34.
49. Gasparro, F. P., Havre, P. A., Olack, G. A., Gunther, E. J., and Glazer, P. M. (1994) *Nucleic Acids Res. 22*, 2845−2852.
50. Takasugi, M., Guendouz, A., Chassignol, M., Decout, J. L., Lhomme, J., Thuong, N. T., and Helene, C. (1991) *Proc. Natl. Acad. Sci. U.S.A. 88*, 5602−5606.
51. Shi, Y. B., Gamper, H., and Hearst, J. E. (1987) *Nucleic Acids Res. 15*, 6843−6854.
52. Averbeck, D. (1985) *Mutat. Res. 151*, 217−233.
53. Degols, G., Clarenc, J. P., Lebleu, B., and Leonetti, J. P. (1994) *J. Biol. Chem. 269*, 16933−16937.
54. Macaulay, V. M., Bates, P. J., McLean, M. J., Rowlands, M. G., Jenkins, T. C., Ashworth, A., and Neidle, S. (1995) *FEBS Lett. 372*, 222−228.
55. Giovannangeli, C., Diviacco, S., Labrousse, V., Gryaznov, S., Charneau, P., and Helene, C. (1997) *Proc. Natl. Acad. Sci. U.S.A. 94*, 79−84.
56. Guieysse, A. L., Praseuth, D., Grigoriev, M., Harel-Bellan, A., and Helene, C. (1996) *Nucleic Acids Res. 24*, 4210−4216.
57. Bates, P. J., Macaulay, V. M., McLean, M. J., Jenkins, T. C., Reszka, A. P., Laughton, C. A., and Neidle, S. (1995) *Nucleic Acids Res. 23*, 4283−4289.
58. Musso, M., Wang, J. C., and Van Dyke, M. W. (1996) *Nucleic Acids Res. 24*, 4924−4932.
59. Faucon, B., Mergny, J. L., and Helene, C. (1996) *Nucleic Acids Res. 24*, 3181−3188.
60. Kandimalla, E. R., Manning, A. N., Venkataraman, G., Sasisekharan, V., and Agrawal, S. (1995) *Nucleic Acids Res. 23*, 4510−4517.
61. Barawkar, D. A., and Bruice, T. C. (1998) *Proc. Natl. Acad. Sci. U.S.A. 95*, 11047−11052.
62. Espinas, M. L., Jimenez-Garcia, E., Martinez-Balbas, A., and Azorin, F. (1996) *J. Biol. Chem. 271*, 31807−31812.
63. Brown, P. M., and Fox, K. R. (1996) *Biochem. J. 319*, 607−611.
64. Svinarchuk, F., Cherny, D., Debin, A., Delain, E., and Malvy, C. (1996) *Nucleic Acids Res. 24*, 3858−3865.
65. Faruqi, A. F., Krawczyk, S. H., Matteucci, M. D., and Glazer, P. M. (1997) *Nucleic Acids Res. 25*, 633−640.
66. Lacoste, J., Francois, J. C., and Helene, C. (1997) *Nucleic Acids Res. 25*, 1991−1998.
67. Olivas, W. M., and Maher, L. J., III (1995) *Nucleic Acids Res. 23*, 1936−1941.
68. Nara, H., Ono, A., and Matsuda, A. (1995) *Bioconjugate Chem. 6*, 54−61.
69. Tsukahara, S., Suzuki, J., Hiratou, T., Takai, K., Koyanagi, Y., Yamamoto, N., and Takaku, H. (1997) *Biochem. Biophys. Res. Commun. 233*, 742−747.
70. Brown, P. M., Madden, C. A., and Fox, K. R. (1998) *Biochemistry 37*, 16139−16151.

BI9902743